DIABETIC Medicine

RESEARCH: BASIC SCIENCE SPECIAL ISSUE

Special Issue: Basic Science Special Issue 2022

Loss of tetraspanin-7 expression reduces pancreatic β-cell exocytosis Ca^{2+} sensitivity but has limited effect on systemic metabolism

Kerry McLaughlin[1] | Samuel Acreman[1,2] | Sameena Nawaz[1] | Joseph Cutteridge[1] | Anne Clark[1] | Jakob G. Knudsen[3] | Geoffrey Denwood[1] | Aliya F. Spigelman[4] | Jocelyn E. Manning Fox[4] | Sumeet Pal Singh[5] | Patrick E. MacDonald[4] | Benoit Hastoy[1] | Quan Zhang[1]

[1]Oxford Centre for Diabetes, Endocrinology and Metabolism, University of Oxford, Churchill Hospital, Oxford, UK

[2]Institute of Neuroscience and Physiology, Department of Physiology, Metabolic Research Unit, University of Goteborg, Göteborg, Sweden

[3]Section for Cell Biology and Physiology, Department of Biology, University of Copenhagen, Copenhagen, Denmark

[4]Alberta Diabetes Institute and Department of Pharmacology, University of Alberta, Edmonton, Alberta, Canada

[5]IRIBHM, Université Libre de Bruxelles (ULB), Brussels, Belgium

Correspondence
Benoit Hastoy and Quan Zhang, Oxford Centre for Diabetes, Endocrinology and Metabolism, University of Oxford, Churchill Hospital, Oxford, UK.
Email: benoit.hastoy@ocdem.ox.ac.uk and quan.zhang@ocdem.ox.ac.uk

Abstract

Background: Tetraspanin-7 (Tspan7) is an islet autoantigen involved in autoimmune type 1 diabetes and known to regulate β-cell L-type Ca^{2+} channel activity. However, the role of Tspan7 in pancreatic β-cell function is not yet fully understood.

Methods: Histological analyses were conducted using immunostaining. Whole-body metabolism was tested using glucose tolerance test. Islet hormone secretion was quantified using static batch incubation or dynamic perifusion. β-cell transmembrane currents, electrical activity and exocytosis were measured using whole-cell patch-clamping and capacitance measurements. Gene expression was studied using mRNA-sequencing and quantitative PCR.

Results: *Tspan7* is expressed in insulin-containing granules of pancreatic β-cells and glucagon-producing α-cells. *Tspan7* knockout mice (Tspan7$^{y/-}$ mouse) exhibit reduced body weight and ad libitum plasma glucose but normal glucose tolerance. Tspan7$^{y/-}$ islets have normal insulin content and glucose- or tolbutamide-stimulated insulin secretion. Depolarisation-triggered Ca^{2+} current was enhanced in Tspan7$^{y/-}$ β-cells, but β-cell electrical activity and depolarisation-evoked exocytosis were unchanged suggesting that exocytosis was less sensitive to Ca^{2+}. *TSPAN7* knockdown (KD) in human pseudo-islets led to a significant reduction in insulin secretion stimulated by 20 mM K$^+$. Transcriptomic analyses show that *TSPAN7* KD in human pseudo-islets correlated with changes in genes involved in hormone secretion, apoptosis and ER stress. Consistent with rodent β-cells, exocytotic Ca^{2+} sensitivity was reduced in a human β-cell line (EndoC-βH1) following *Tspan7* KD.

Conclusion: Tspan7 is involved in the regulation of Ca^{2+}-dependent exocytosis in β-cells. Its function is more significant in human β-cells than their rodent counterparts.

Samuel Acreman and Sameena Nawaz have shared equal contribution to the study.

1 | INTRODUCTION

Tetraspanin-7 (Tspan7) was recently established as an autoantigen in type 1 diabetes mellitus (T1D),[1] an autoimmune disease in which loss of pancreatic β-cells leads to chronic hyperglycaemia.[2] Proteins of the tetraspanin superfamily, of which Tspan7 is a member, are characterised by the presence of four transmembrane domains: one short and one long extracellular loop, a short intracellular loop, and N-terminal and C-terminal cytoplasmic tails.[3,4] Tetraspanin proteins are typically organised in tetraspanin-enriched microdomains on biological membranes[5] where they act as molecular facilitators, engaging both transmembrane and intracellular proteins to regulate diverse processes such as cell proliferation, differentiation, activation, adhesion, motility and signalling.[5–7]

Tspan7 is highly expressed in neuroendocrine tissue,[8] and loss of Tspan7 can lead to defects in neuronal morphogenesis and synaptic transmission,[9] similar to those described in people expressing a mutated form.[10] Additional functions in cell morphology have been reported in dendritic cells[11] and osteoclasts,[12] attributed to its role in actin cytoskeleton rearrangement. Within the pancreas, Tspan7 is localised to the pancreatic islets and was recently shown to function as an auxiliary protein of L-type voltage-gated Ca^{2+} channels (VGCCs), modulating β-cell electrical excitability and exocytosis. Knocking-down of *Tspan7* in β-cells led to higher Ca^{2+} influx (through L-type VGCCs), cellular excitability and glucose-stimulated insulin secretion.[13]

In this study, we characterised $Tspan7^{y/-}$ mouse metabolic phenotype, β-cell excitability, glucose-stimulated insulin secretion and cell exocytosis. These data provide further insights of the role of Tspan7 in regulating β-cell intracellular Ca^{2+} dynamics and insulin secretion, and thus to determine the importance of Tspan7 in glucose tolerance.

2 | METHODS

2.1 | Animals and isolation of pancreatic islets

All animal experiments were conducted in accordance with the UK Animals Scientific Procedures Act (1986) and the University of Oxford ethical guidelines. Mouse islets were isolated as previously described.[14,15] *Tspan7* knockout mice ($Tspan7^{y/-}$)[9] were gifts from Dr Luca Murru (CNR Institute of Neuroscience, Milano, Italy). Hormone secretion studies and the electrophysiology experiments

Novelty statement

What is already known?

Tetraspanin-7, a transmembrane protein widely expressed in pancreatic islet cells, was previously identified as an autoantigen in type 1 diabetes. Tetraspanin-7 has been shown to regulate β-cell L-type Ca^{2+} channel activity.

What did this study find?

Genetic ablation of tetraspanin-7 in mice led to a significant reduction in the Ca^{2+} dependence of β-cell exocytosis. This phenotype was also observed in human islet cells following ex vivo tetraspanin-7 knockdown, alongside down-regulation of the β-cell exocytosis Ca^{2+} sensor, synaptotagmin-7.

What are the implications of the study?

Tetraspanin-7 expression is required for normal exocytotic machinery and appropriate exocytosis Ca^{2+} sensitivity in pancreatic β-cells.

were performed on islets isolated from $Tspan7^{y/-}$ mice and their wildtype littermates (control).

2.2 | shRNA

Adenoviruses expressing shRNA for silencing of human TSPAN7 (Ad-ShTSPAN7, SKU# shADV-226,651) or scrambled shRNA control (Ad-Scramble, SKU# 1122) together with eGFP under a CMV promoter were purchased from Vector Biolabs.

2.3 | Human pseudo-islets and EndoC-βH1 cell line

Donor organs were obtained with written consent and research ethics approval at the University of Alberta, and human islets were isolated as previous described[16] at the University of Alberta. All human islet information is listed in Table S1. Islets were dispersed into a single-cell suspension using trypsin (TryLE Express, Gibco) and transduced with Ad-ShTSPAN7 or Ad-Scramble before

forming human pseudo-islets using centrifugal-forced aggregation as previously described.[17] EndoC-βH1 was provided by Endocell and cultured as previously described.[18]

2.4 | Insulin secretion

Insulin secretion was measured in static incubations as previously described.[15] Briefly, groups of 10–20 isolated islets (number depended on islet availability) were preincubated for 30 min at 37°C in Krebs-Ringer buffer (KRB) consisting of (mM): 140 NaCl, 3.6 KCl, 0.5 MgSO$_4$, 2.6 CaCl$_2$, 0.5 NaH$_2$PO$_4$, 2 NaHCO$_3$, 1 glucose and 5 HEPES (pH = 7.4 with NaOH), before being incubated for 60 min at 37°C in 1 ml of KRB supplemented as indicated in the legends. Immediately after incubation, an aliquot of the medium was removed for determination of insulin concentration using an ELISA kit (Mercodia, Sweden).

For dynamic insulin secretion measurements, groups of 50 pseudo-islets were perifused with KRB containing 1 or 16.7 mM glucose with or without 20 mM K$^+$ (as indicated) at the rate of 100 μl/min, using a perifusion system (Biorep, FL, USA). Perfusate was collected every 2 min and insulin concentration was determined using the Alpco stellux human ELISA kits (Salem, NH).

The perifusion experiments were conducted at the University of Alberta and the mRNAs of pseudo-islets were then extracted using TRIzol (ThermoFisher) before shipped to Oxford for transcriptomic study.

EndoC-βH1 cells were sequentially exposed for 20 min to 1 and 20 mM glucose containing KRB. Supernatants were collected at the end of each incubation and insulin cellular contents were extracted using acid ethanol. Insulin concentrations were determined using an ELISA kit (Mercodia, Sweden).

2.5 | Electrophysiology

Electrophysiological measurements were performed using an EPC-10 patch-clamp amplifier and Pulse software (version 8.80, HEKA Electronics, Germany). Electrical activity and K$_{ATP}$-channel conductance were measured using perforated patch-clamping technique as previously described[19]; membrane currents and changes in cell capacitance were recorded using voltage clamp in combination with capacitance measurements, as described in.[14] β-cells were identified by electrophysiological fingerprinting.[20]

2.6 | Histology

Sections of formalin-fixed paraffin-embedded tissue were de-waxed and subjected to epitope retrieval in a microwave pressure cooker in 10 mM citric acid pH 6.0, 0.05% Tween 20. After blocking with 2.5% normal horse serum, sections were incubated overnight (4°C) with rabbit anti-Tspan7 antibody (Anti-TM4SF2, 1:50, Sigma-Aldrich). Antibody labelling was detected with the VectaFluor™ Excel Amplified Anti-Rabbit IgG, DyLight™ 488 Antibody Kit (Vector Laboratories). Slides were counterstained with guinea pig anti-insulin (1:500, Dako) and mouse anti-glucagon (1:500, Sigma) antibodies followed by labelling with goat anti-guinea pig-Alexa 633 (1:100) and goat anti-mouse Alexa 555 (1:100) secondary antibodies (ThermoFisher). Slides were visualised by confocal microscopy.

For electron microscopy, isolated human islets were fixed in 2.5% glutaraldehyde in PBS, postfixed in 1% OsO4, dehydrated and embedded in Spurr's resin. Sections were cut onto nickel grids before being immunolabelled using anti-TM4SF2 (1:20) and protein A gold particles (15 nm, Biocell), guinea pig anti-insulin antibody (DAKO, 1:500) followed by anti-guinea pig gold 10 nm (British Biocell International), and mouse anti-glucagon (1:500, Sigma) followed by anti-mouse pig gold 10 nm (British Biocell International). Sections were viewed with a Joel 1010 microscope (accelerating voltage 80 kV).

To establish the specificity of Tspan7 antibody, immunostaining was conducted using a stable *Tspan7* KD INS-1 cell line (cell line generation is described in Data S1). *Tspan7* KD INS-1 or control cells were fixed in 4% PFA, permeabilised using 0.1% Triton X-100 and blocked with 5% normal swine serum. Tspan7 was detected using rabbit anti-Tspan7 primary antibody (anti-TM4SF2, 1:50, Sigma-Aldrich; overnight incubation, 4°C), and with goat anti-rabbit IgG Alexa Fluor 568 secondary antibody (Life Technologies). Nucleus were stained with RedDot2 (BioTium; 1:200 dilution). Slides were visualised by confocal microscopy (BioRad).

2.7 | Glucose tolerance test

Intraperitoneal (i.p.) glucose tolerance test was performed as previously described.[15] Briefly, the animals were individually fasted for 6 h before i.p. injected with a bolus of glucose (2 g/kg body weight). Blood glucose were monitored for 90 min using a glucometer by tail vein sampling.

2.8 | quantitative PCR

RNA was extracted from human pseudo-islets using TRIzol Reagent (Life Technologies, 15,596,026) according to the manufacturer's instructions. cDNA was generated using the GoScript Reverse Transcription Kit (Promega,

A5000). qPCR was performed using 20 ng of cDNA, and TaqMan Gene Expression Master Mix (Life Technologies Ltd, 4,369,016) or SYBR™ Green PCR Master Mix (Applied Biosystems, 4,309,155) with the gene expression assays or primers as detailed in Table 1. Gene expression was determined using the ΔΔCT method by normalising to HouseKeeping Genes (HKG) and to the level of expression of each target detected in Ad-Scramble transduced cells. Data are presented as percentage of control.

2.9 | RNA sequencing

Human pseudo-islets were preserved in Trizol before their total RNA was extracted using Quick-RNA MicroPrep kit (R1050 Zymo Research). RNA libraries for RNA-seq were prepared using NEBNext Ultra II Directional RNA Library Prep Kit for Illumina following manufacturer's protocols. Sequencing was performed on NextSeq 550. Single-end reads were splice-aligned to a human genome (GRCh38) using GSNAP. FeatureCounts was used to assign reads to exons thus eventually getting counts per gene. EdgeR package of R[21] was used to perform differential analysis between the conditions (shRNA vs control), while controlling for the confounding effect from the donor. Across-samples normalisation was performed using the TMM normalisation method.

2.10 | Data analyses and statistics

Data are expressed as mean value $\pm$ SEM. p-values less than 0.05 were considered significant. Statistical analyses were performed using OriginPro 2017 either by Student's t-test, paired comparison or two-way ANOVA and Tukey post hoc test. Ns represent the number of cells for electrophysiological analyses, and of independent mice or cell passages for hormone assays and expression data.

3 | RESULTS

3.1 | *Tspan7* is expressed in pancreatic islets

Tspan7 expression in pancreatic islets was evaluated using immunohistochemistry. In both human and mouse pancreatic islets, Tspan7 was found to colocalise with insulin and glucagon, confirming its expression in β- and α-cells[13] (Figure 1a). We observed enriched immunogold labelling of Tspan7 in large dense-core vesicle of human α- and β-cells (Figure 1b,c), consistent with a previous report that Tspan7 was present in the cytoplasm of islet cells with a distribution pattern similar to islet hormones.[22]
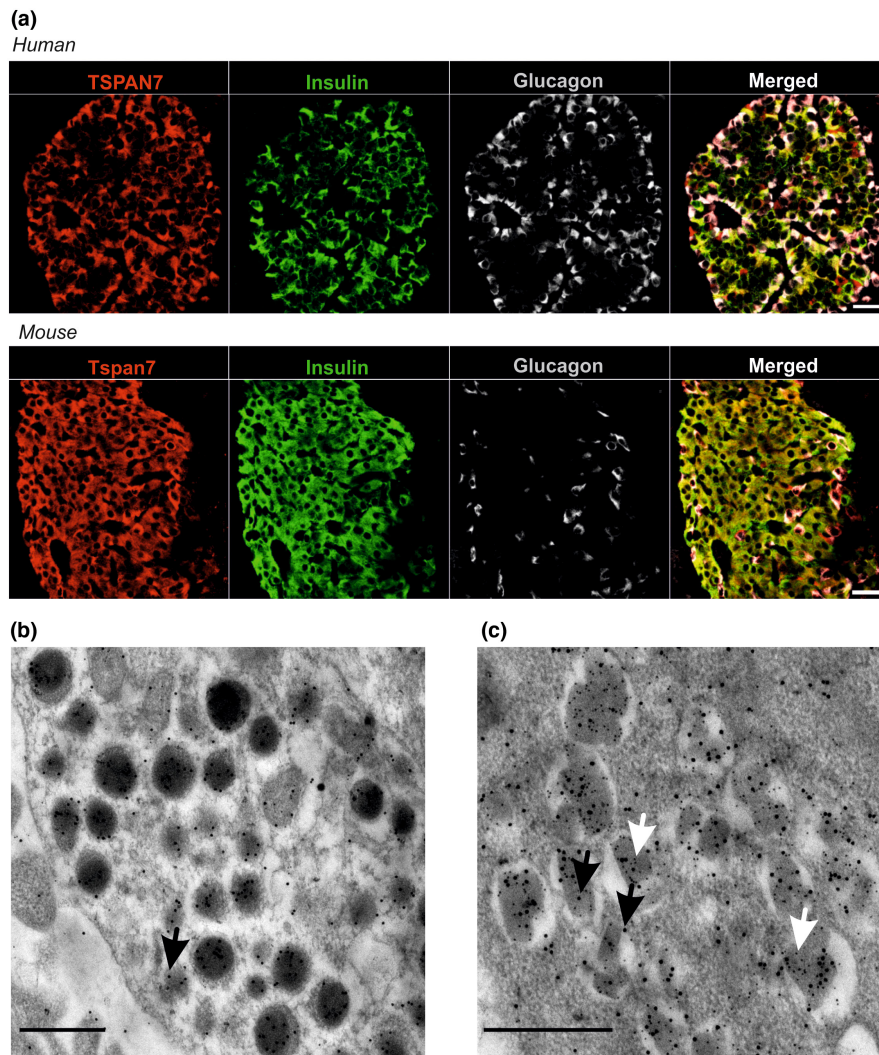
3.2 | Ablation of *Tspan7* has limited impact on glucose tolerance

To investigate the role of Tspan7 in islet function and systemic metabolism, a *Tspan7* knockout mouse model (Tspan7$^{y/-}$)[9] was used. Reduced body weight and ad libitum plasma glucose was observed in Tspan7$^{y/-}$ mice (Figure 2a,b), but this was not linked to changes in plasma insulin (measured as insulin and C-peptide, Figure 2c,d). These effects may instead be attributable to the neurological manifestations of *Tspan7* ablation, including depressive behaviour.[23] We observed no change in circulating proinsulin levels (Figure 2e), suggesting normal insulin

TABLE 1 Primers and types of assays used for quantitative PCR analyses

Gene symbol	Gene name	Assay ID	Supplier
ACTB	Actin, Beta (HKG)	Hs01060665_g1	Life Technologies Ltd
B2M	Beta-2-microglobulin (HKG)	Hs00187842_m1	Life Technologies Ltd
GAPDH	Glyceraldehyde-3-phosphate dehydrogenase (HKG)	Hs02786624_g1	Life Technologies Ltd
SYT 4	Synaptotagmin 4	Hs01086433_m1	Life Technologies Ltd
SYT 5	Synaptotagmin 5	Hs01100015_g1	Life Technologies Ltd
SYT 7	Synaptotagmin 7	Hs01590513_m1	Life Technologies Ltd
CACNA1A	Calcium voltage-gated channel subunit alpha1 A	Hs01579431_m1	Life Technologies Ltd
CACNA1C	Calcium voltage-gated channel subunit alpha1 C	Hs00167681_m1	Life Technologies Ltd
CACNA1D	Calcium voltage-gated channel subunit alpha1 D	Hs00167753_m1	Life Technologies Ltd
TSPAN7	Tetraspanin 7	Hs_TSPAN7_1_SG QT00052010	Qiagen QuantiTect

processing in Tspan7$^{y/-}$ β-cells. Furthermore, when subjected to intra-peritoneal glucose tolerance tests (IPGTTs), no difference in glucose tolerance (Figure 2f) or glucose-induced insulin secretion (GSIS, Figure S1) was observed between Tspan7$^{y/-}$ and control mice.

3.3 | Exocytosis sensitivity to Ca^{2+} was reduced in Tspan7$^{y/-}$ β-cells

In β-cells, glucose metabolism increases the intracellular ATP/ADP ratio, resulting in closure of ATP-sensitive K$^+$ channels (K$_{ATP}$-channels) inducing membrane depolarisation and action potential (AP) firing. APs open voltage-gated Ca^{2+} channels (VGCCs), enabling influx of Ca^{2+} to trigger Ca^{2+}-dependent exocytosis, culminating in insulin secretion. To interrogate the impact of *Tspan7* ablation on β-cell function at a single-cell level, we phenotyped Tspan7$^{y/-}$ β-cell excitability, transmembrane Ca^{2+} currents and exocytosis using electrophysiological techniques. In the presence of 1 mM glucose, Tspan7$^{y/-}$ and

control β-cells were both repolarised (Tspan7$^{y/-}$ vs. control: -80 ± 1 mV vs. -80 ± 2 mV; $p = 0.4$) and electrically silent. Elevating extracellular glucose or blocking the K$_{ATP}$ channels (using tolbutamide, 200 μM) induced membrane depolarisation and firing of APs in β-cells of both genotypes (Figure 3a). In the presence of 10 mM glucose, although the Tspan7$^{y/-}$ β-cells were less depolarised (Tspan7$^{y/-}$ vs. control: -57 ± 4 mV vs. -46 ± 5 mV; $p < 0.05$), no difference in AP peak or firing frequency was observed across the two genotypes (Figure 3b–d). There was no apparent difference in AP halfwidth or spike duration, either (Figure S2). Further increasing extracellular glucose to 20 mM or inhibiting K$_{ATP}$ channels with tolbutamide exerted similar effects on the electrical activity of both Tspan7$^{y/-}$ and control β-cells (Figure 3b–d). However, Tspan7$^{y/-}$ β cells responded to 20 mM glucose stimulation faster than the control (Tspan7$^{y/-}$ vs. control: 2.4 ± 0.3 min vs. 3.85 ± 0.3 min, $p < 0.05$). These marginal changes in Tspan7$^{y/-}$ β-cell electrical activity are not due to any apparent changes in K$_{ATP}$-channel conductivity or glucose sensitivity (Figure 3e,f).

Transient knockdown of Tspan7 in β-cells was recently shown to increase Ca^{2+} influx through L-type VGCC.[13] We assessed whether a similar phenotype can be observed in β-cells of mice with a constitutive *Tspan7* knockout. As shown in Figure 4a,b, depolarisation triggered a significantly larger Ca^{2+} current in Tspan7$^{y/-}$ β-cells than in the control ($p < 0.01$, ~160% at 0 and 10 mV), consistent with Dickerson et al.[13] As Ca^{2+} triggers exocytosis, we tested whether enhanced VGCC activity led to higher exocytosis in Tspan7$^{y/-}$ β-cells using capacitance measurements. Exocytosis (measured as increases in cell capacitance) was trigged by a series of depolarising pulses from −70 mV to 0 mV with progressively longer durations (from 10 ms to 800 ms). Unexpectedly, exocytosis was comparable between Tspan7$^{y/-}$ and control β-cells at all pulse durations (Figure 4c,d). We correlated the Ca^{2+} charges (total influx Ca^{2+} ions, QCa^{2+}) with the corresponding exocytosis elicited by depolarisation (Figure 4e). Whereas exocytosis could be triggered by 0.15 pC/pF QCa^{2+} in control β-cells, it required > ~ 0.2 pC/pF in Tspan7$^{y/-}$ β-cells, suggesting a reduced exocytotic Ca^{2+} sensitivity.

Given the limited changes in electrical activity and exocytosis in Tspan7$^{y/-}$ β-cells, we reasoned that knocking-out *Tspan7* would have little effect on glucose/tolbutamide-stimulated insulin secretion. Indeed, no significant difference was observed in insulin secretion, stimulated by 10 mM glucose or 0.2 mM tolbutamide, from islets of control and Tspan7$^{y/-}$ mice (Figure 4f). We reasoned that enhanced VGCC activity augments the concentration of cytosolic Ca^{2+}, and thus may induce apoptosis,[24] affecting islet β cell mass in aged animals. However, no significant difference in GSIS, insulin secretion induced by 70 mM K^+ or islet insulin content was observed in control and Tspan7$^{y/-}$ islets isolated from 1-year-old mice (Figure S4).

3.4 | Reducing *TSPAN7* expression in human islets changes gene expression of islet exocytosis Ca^{2+} sensors

To assess the role of tetraspanin-7 in human β-cell function, we utilised an adenovirus encoding shRNATSPAN7
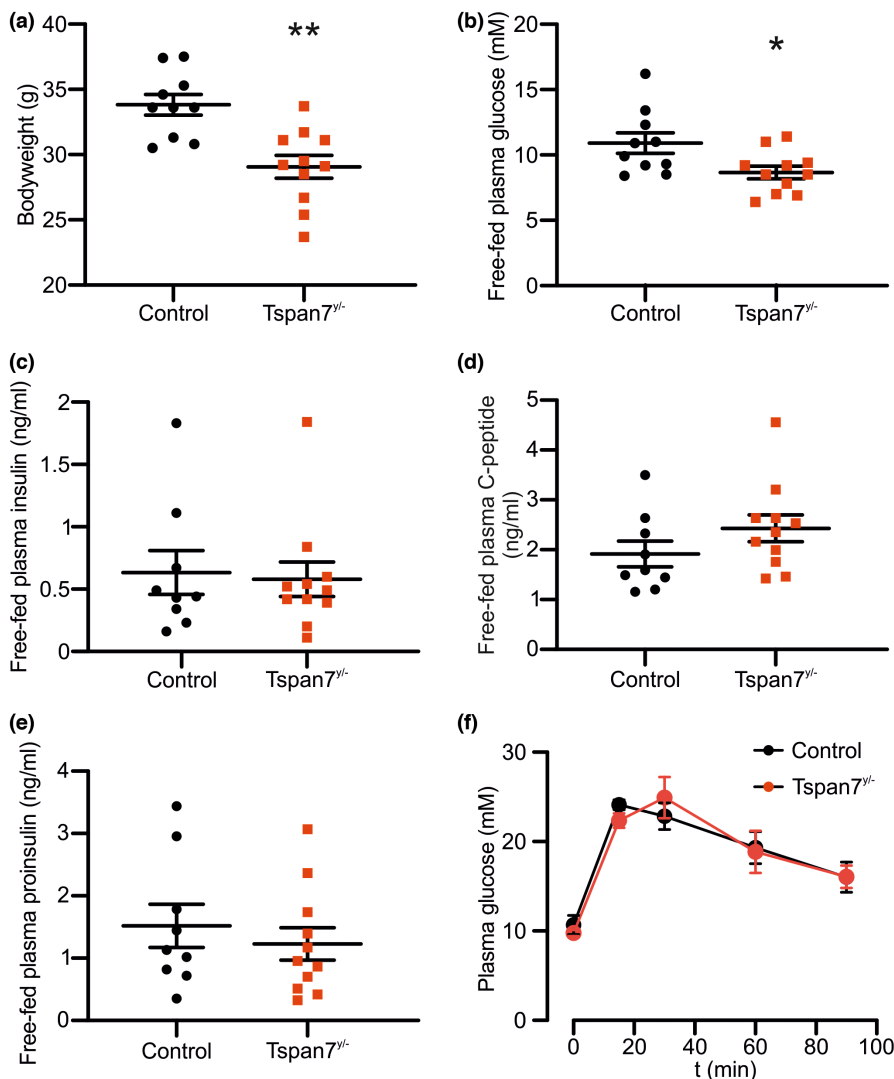

FIGURE 2 In vivo metabolic phenotyping of Tspan7$^{y/-}$ mouse model. (a–e) Ad libitum bodyweight (a), and plasma concentrations of glucose (b), insulin (c), C-peptide (d) and proinsulin measured in Tspan7$^{y/-}$ mice (red) and age-matched (11.3 ± 0.3 wks) litter mate control (black). *$p < 0.05$ versus control and **$p < 0.01$ versus control. (f) Plasma glucose concentrations of Tspan7$^{y/-}$ mice (red) and age-matched litter mate control (black) measured during intraperitoneal glucose tolerance tests. Glucose bolus was injected at 0 min. $N = 5$ for control and 6 for Tspan7$^{y/-}$. Data are presented as mean value ± SEM.
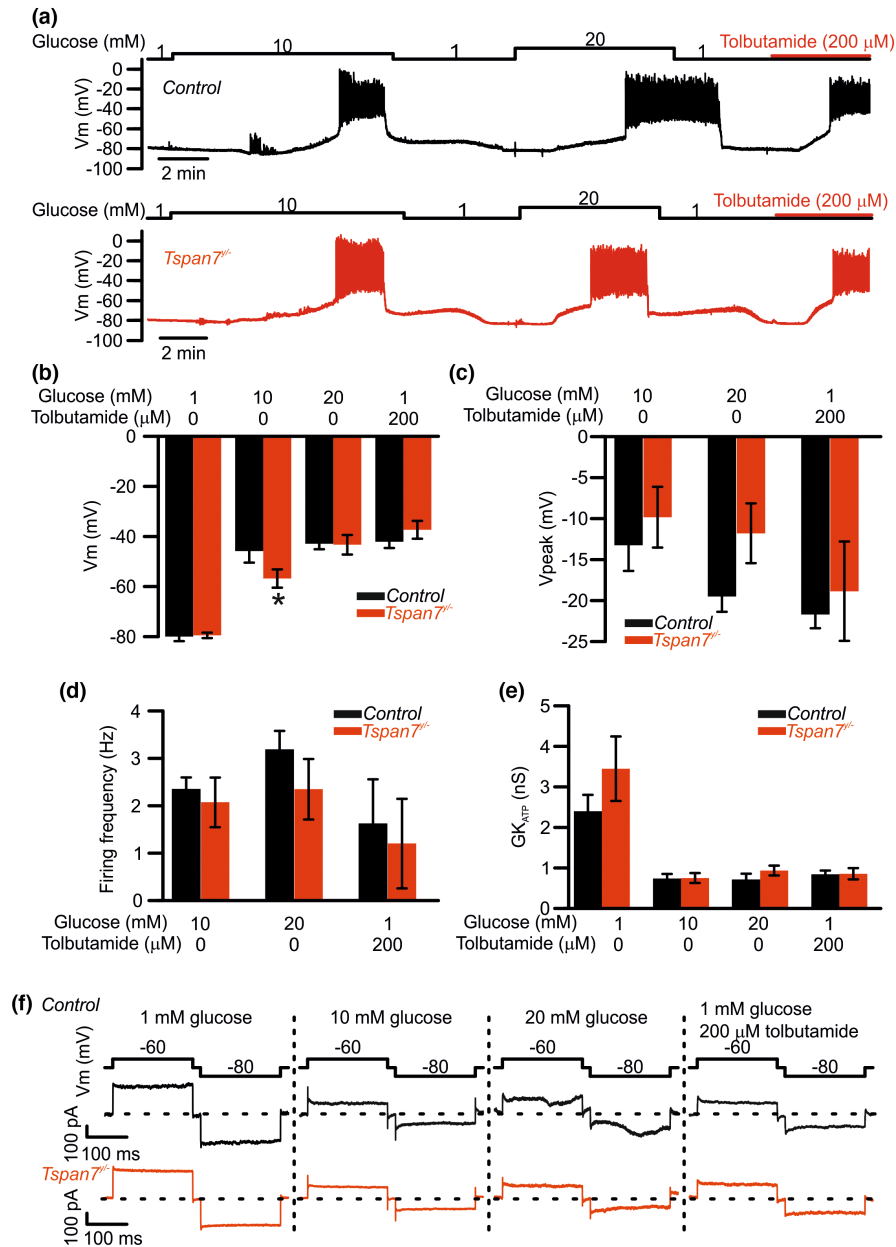
FIGURE 3 Electrical activity and K_{ATP}-channel conductance measured in Tspan7$^{y/-}$ β-cells. (a) Membrane potential recordings of control (upper trace, black) and Tspan7$^{y/-}$ (lower trace, red) β-cells within intact islets in response to changes in extracellular glucose (1 mM, 10 mM and 20 mM) or application of 200 μM tolbutamide, as indicated. (b) Summary of control (black) and Tspan7$^{y/-}$ (red) β-cell membrane potential measured at conditions indicated. $N = 7$ for control and 14 for Tspan7$^{y/-}$ β-cells at 1 mM glucose; $N = 7$ for control and 11 for Tspan7$^{y/-}$ β-cells at 10 mM glucose; $N = 4$ for control and 6 for Tspan7$^{y/-}$ β-cells at 20 mM glucose and $N = 3$ for control and 6 for Tspan7$^{y/-}$ β-cells when 200 μM tolbutamide was applied. *$p < 0.05$ versus control. (c, d), as in (b) but summarise the peak voltage (c) and firing frequency (d) of action potentials measured in control (black) and Tspan7$^{y/-}$ (red) β-cells at conditions indicated. $N = 4$ for control and 7 for Tspan7$^{y/-}$ β-cells at 10 mM glucose; $N = 4$ for control and 6 for Tspan7$^{y/-}$ β-cells at 20 mM glucose and $N = 3$ for control and 3 for Tspan7$^{y/-}$ β-cells when tolbutamide was applied. (e) Summary of K_{ATP}-channel conductance measured in control (black) and Tspan7$^{y/-}$ (red) β-cells under the conditions indicated. $N = 4$ for control and 7 for Tspan7$^{y/-}$ β-cells at 1 mM and 10 mM glucose; $N = 4$ for control and 6 for Tspan7$^{y/-}$ β-cells at 20 mM glucose and $N = 3$ for control and 5 for Tspan7$^{y/-}$ β-cells when tolbutamide was applied. (f) Examples of K_{ATP} currents measured in control (black, middle trace) and Tspan7$^{y/-}$ (red, bottom trace) β-cells. K_{ATP} currents were triggered by ±10 mV excursions from -70 mV (200 ms, top) in voltage-clamped β-cells under the conditions indicated. All data are presented as mean value $\pm$ SEM.

(Ad-ShTSPAN7) to knockdown (KD) human *TSPAN7* expression. Islet cells transduced with Ad-ShTSPAN7, or the control virus (with scrambled RNA), were used to form pseudo-islets. RNA sequencing showed a marked reduction in *TSPAN7* expression (92.65%) in the *TSPAN7*-KD pseudo-islets (log$_2$[Fold-change] = -3.765,
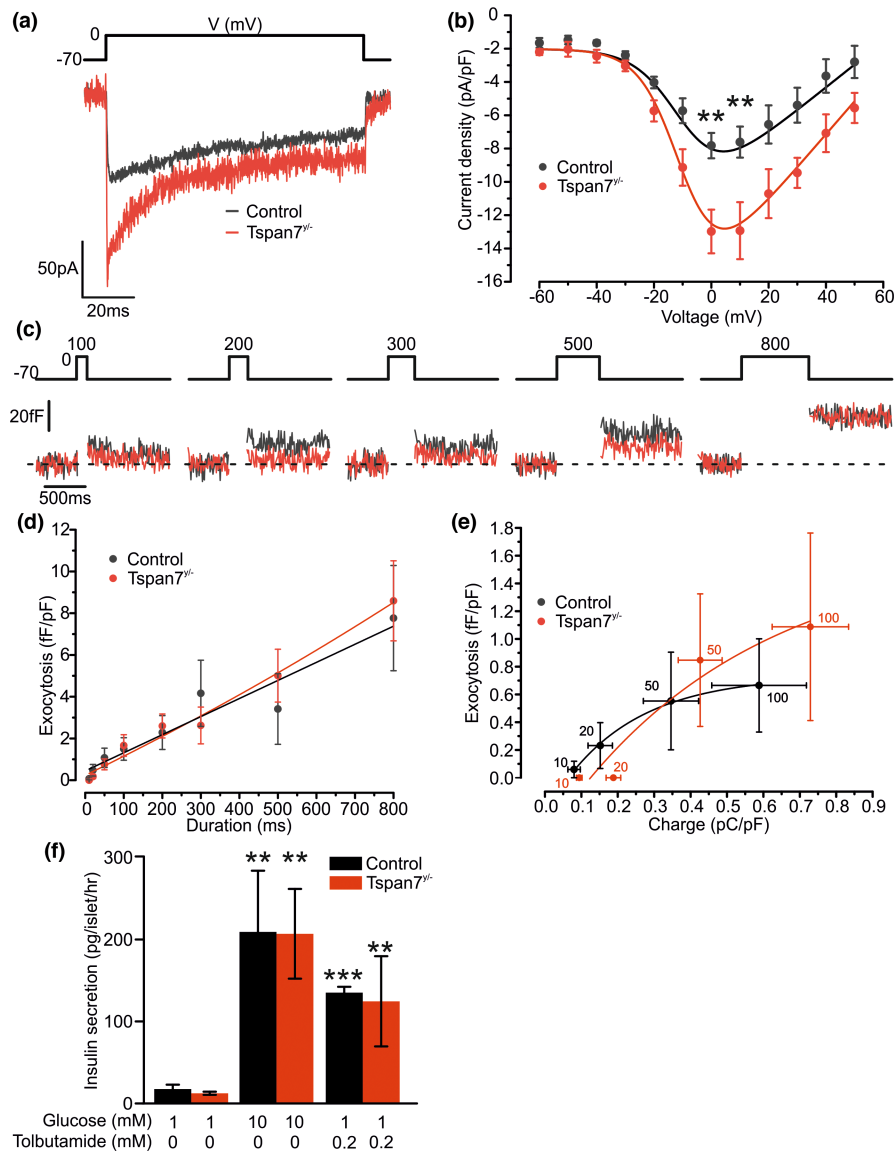
FIGURE 4 Ca^{2+} current and exocytosis in Tspan7$^{y/-}$ β-cells. Tspan7 loss of function significantly increases Ca^{2+} current density in β cells (a, b). (a) Representative traces of control (black) and Tspan7$^{y/-}$ (red) β-cell Ca^{2+} current elicited by a 100-ms depolarisation from −70 mV to 0 mV. (b) Summary of control (black) and Tspan7$^{y/-}$ (red) β-cell Ca^{2+} current density in relationship to membrane voltages. $N = 7$ for control and 5 for Tspan7$^{y/-}$ β-cells, **$p < 0.01$ versus control, paired comparison and Tukey. (c) Examples of exocytosis induced by membrane depolarisations from −70 mV to 0 mV (at the duration of 100 ms, 200 ms, 300 ms, 500 ms and 800 ms as indicated above the traces) of control (black) and Tspan7$^{y/-}$ (red) β-cells. (d) Summary of control (black) and Tspan7$^{y/-}$ (red) β-cell exocytosis (normalised to cell size, fF/pF) in relationship to pulse durations. $N = 11$ cells for control and 14 cells for Tspan7$^{y/-}$ β-cell. (e) Control (black) and Tspan7$^{y/-}$ (red) β-cell charges-exocytosis relationship for pulses up to 100 ms. Corresponding durations of the pulses are as labelled. $N = 7$ cells for control and 5 cells for Tspan7$^{y/-}$ β-cells. (f) Insulin secretion measured from batch-incubated control (black) and Tspan7$^{y/-}$ (red) islets in response to glucose or tolbutamide (concentrations as indicated). Islets were isolated from mice aged 20 weeks and N ≥ 3 for control and Tspan7$^{y/-}$ islets. **$p < 0.01$ and ***$p < 0.001$ versus 1 mM glucose alone of the same genotype. All data are presented as mean value ± SEM.

p_{adj} = 6.42 E-13) (Figure 5a), confirming successful genetic manipulation. In total, 1030 genes (1000 are protein-coding genes) were down-regulated and 395 genes (372 are protein-coding genes) were up-regulated in *TSPAN7*-KD pseudo-islets. Pathway analyses showed up-regulation in apoptosis gene ontology pathway (p_{adj} = 4.08 E^{-7}); and down-regulation of genes involved in the secretory

pathway and transport regulation (p_{adj} = 5.62 E^{-9} and 4.22 E^{-08} respectively). Interestingly, β-cell expression of the exocytosis Ca^{2+} sensor *SYT7* was reduced in *TSPAN7*-KD pseudo-islets (log$_2$[Fold-change] = −0.39, p_{adj} = 3.89 E^{-3}). GSIS of the pseudo-islets were tested using dynamic perifusion experiments (Figure 5b). Whereas insulin secretion at basal or 16.7 mM glucose

was comparable between the *TSPAN7*-KD and control pseudo-islets, 20 mM K^+-stimulated insulin secretion was significantly lower in *TSPAN7*-KD pseudo-islets.

The insulin secretion experiments suggested that *TSPAN7* may play a role in human β-cell exocytosis. To test this, we performed capacitance measurements using EndoC-βH1, a human β-cell line recapturing functional and genetic features of primary human β-cells,[18] transduced with Ad-ShTSPAN7 or Ad-Scramble virus. Similar to that observed in mouse Tspan7$^{y/-}$ β-cells, exocytosis triggered by depolarisation was comparable between *TSPAN7*-KD EndoC-βH1 and control cells (Figure 5c,d). However, depolarisation triggered larger influx of charges ($p < 0.05$) in *TSPAN7*-KD EndoC-βH1 cells than that of the control (Ad-Scramble) (Figure 5e). Importantly, the exocytotic Ca^{2+}-sensitivity of *TSPAN7*-KD EndoC-βH1 was reduced (same QCa^{2+} could only evoke exocytosis that was ~50% of the control, Figure 5f). This correlated with a significantly reduced GSIS in *TSPAN7*-KD EndoC-βH1 ($p < 0.01$, Figure 5g) without affecting insulin content (Figure 5h). We measured the changes in gene expression of VGCC and synaptotagmins in *TSPAN7*-KD EndoC-βH1. Concomitantly to *TSPAN7* KD ($p = 5.51 \, E^{-4}$), *CACNA1A* was up-regulated and *SYT5* and *SYT7* were down-regulated (-20%, Figure 6).
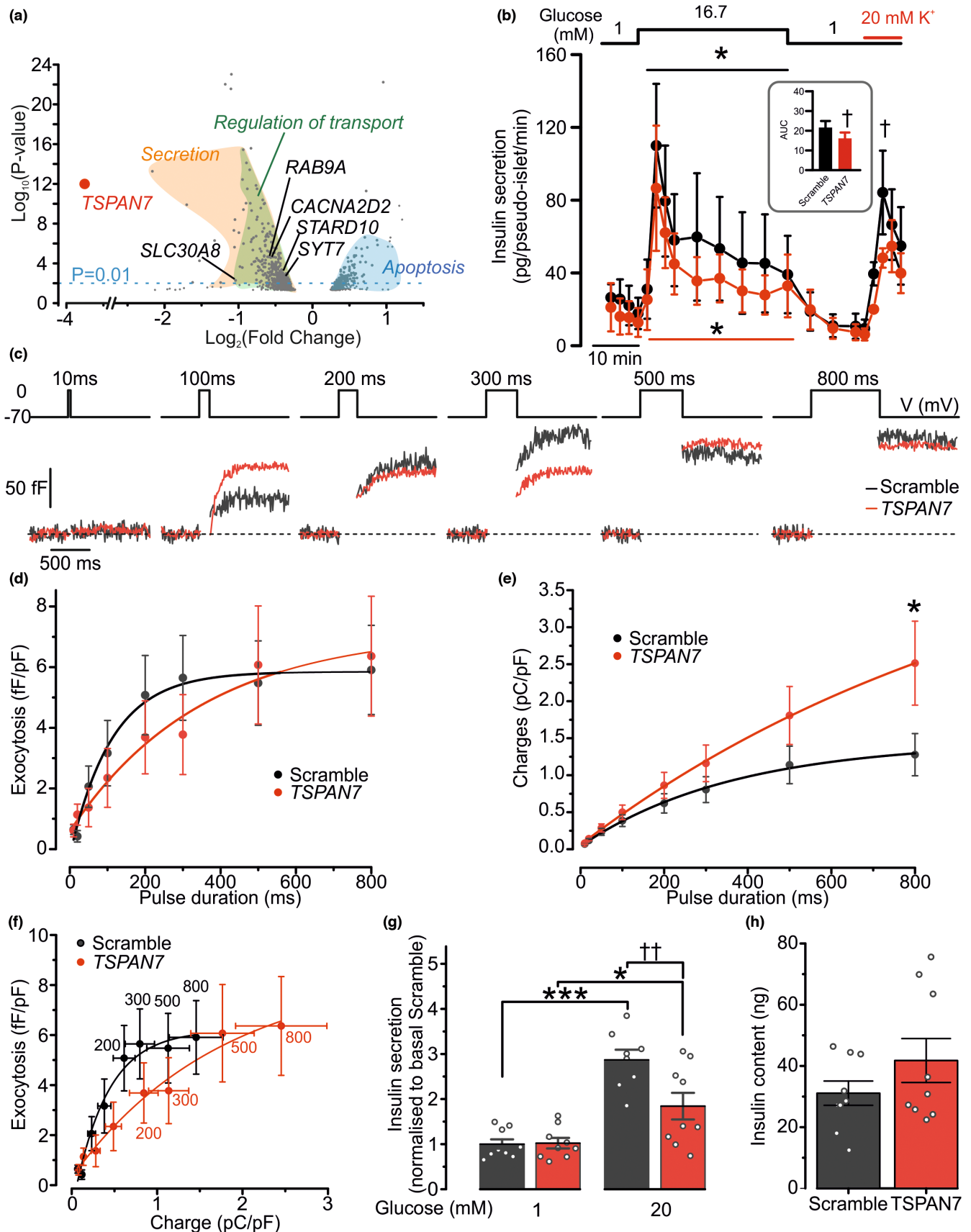
4 | DISCUSSION

Autoantigens implicated in type 1 diabetes have been shown to play a role in the regulation of insulin secretion.[25] Tspan7, a recently identified T1D autoantigen, can interact with both intracellular and membrane proteins, regulating diverse cellular processes, in a variety of cell types.[5] While Tspan7 expression in β-cells is well established,[8,13,22] its role in insulin secretion is only partially understood. Here, we show that, in addition to its role in regulating VGCCs,[13] adequate expression of *Tspan7* is required to maintain Ca^{2+} sensitivity of β-cell exocytosis, which is associated with appropriate expression of synaptotagmin 7. This correlation is found in both mouse and human β-cells but exerts a more significant role in human β-cell function.

The role of Tspan7 in regulating cellular functions has been studied in many different cell types[5,6,9,10,12,23] and this has been recently extended into the study of pancreatic β-cells,[13] where it was found to reduce L-type VGCC activity. Therefore, reducing *Tspan7* expression in β-cells would be expected to lead to higher Ca^{2+} influx, improving glucose tolerance through enhanced GSIS (a Ca^{2+}-dependent process). Indeed, in Tspan7$^{y/-}$ β-cells, depolarisation-triggered Ca^{2+} current was augmented (Figure 4a; Figure S3a) and this may contribute to the

trend of increased action potential peak, decreased inter-spike plateau potential and lower firing frequency at high glucose (Figure 3b–d), similar to the effect of an L-type VGCC agonist BAYK 8644.[26] However, this increment ($\sim +3$ pA/pF at 0 mV) did not significantly change β-cell action potential (Figure S1) and thus, may not be sufficient to impact on insulin secretion. This is confirmed by the normal GSIS observed in Tspan7$^{y/-}$ mice, both in vivo (Figure S1) and in vitro (Figure 4f). Similarly, GSIS was not significantly altered in human pseudo-islets transduced with *TSPAN7* shRNA. This differs from the previous report by Dickerson et al.[13] and may result from the different experimental paradigms used across the two studies (i.e., 2D single cell culture or 3D pseudo-islets). Pseudo-islets, formed by re-aggregating dispersed islet cells, is an approximation of the primary intact islet, preserving a more physiological environment that includes intra-islet paracrine signalling. Pseudo-islet function is comparable with primary human islets[17] and allows efficient genetic manipulation using transduction, as highlighted in the present study (Figure 5a).

The stimulus-secretion coupling of β-cells involves exocytosis that depends on Ca^{2+} influx through the L-type VGCC.[14] However, the observation that depolarisation-triggered insulin secretion was unaffected in Tspan7$^{y/-}$ islets (Figure 4f; Figure S4) and slightly reduced in *TSPAN7* KD human pseudo-islets (Figure 5b) suggests reduced Tspan7/TSPAN7 may also affect exocytotic machinery. By correlating the transmembrane Ca^{2+} influx with high-resolution exocytosis measurements, it is clear that exocytosis Ca^{2+} sensitivity is impaired when the level of tetraspanin-7 in β-cells is low. This effect could be in part attributed to reduced expression of *Syt7*, the major β-cell exocytosis Ca^{2+} sensor.[27] Down-regulation of the *Syt7* following tetraspanin-7 ablation/knockdown may be due to: (1) a coordinated expressions of these genes, or (2) Ca^{2+}-dependent changes in gene expression (secondary to augment VGCC activity, reviewed in[28]). Either possibility suggests that expression of tetraspanin-7 may be required for appropriate assembly of exocytotic machinery in β-cells. It is therefore likely that TSPAN7 plays a more significant role in insulin secretion in human β-cells, in which exocytosis is less dependent on L-type VGCC (more P/Q-type VGCC dependent[29]). This notion is consistent with the observation that insulin secretion induced by 20 mM K^+ and GSIS was reduced in *TSPAN7* KD pseudo-islets and EndoC-βH1 cells respectively (Figure 5b,g). It is interesting to note that the impact of *TSPAN7* KD on pseudo-islets GSIS is less pronounced. This highlights the difference between the primary islets or reconstituted organoids and human cell lines. Whereas the primary human islets (and the pseudo-islets) are comprised of different type of endocrine cells, EndoC-βH1 cells

(a) Log₁₀(P-value) vs Log₂(Fold Change). Regulation of transport, Secretion, TSPAN7, RAB9A, CACNA2D2, STARD10, SYT7, SLC30A8, Apoptosis, P=0.01.

(b) Insulin secretion (pg/pseudo-islet/min) vs time. Glucose (mM) 1, 16.7, 1, 20 mM K⁺. Scramble vs TSPAN7. Inset: AUC.

(c) 10ms, 100ms, 200 ms, 300 ms, 500 ms, 800 ms pulse traces. Scramble, TSPAN7.

(d) Exocytosis (fF/pF) vs Pulse duration (ms). Scramble, TSPAN7.

(e) Charges (pC/pF) vs Pulse duration (ms). Scramble, TSPAN7.

(f) Exocytosis (fF/pF) vs Charge (pC/pF). Scramble, TSPAN7.

(g) Insulin secretion (normalised to basal Scramble) vs Glucose (mM) 1, 20.

(h) Insulin content (ng). Scramble, TSPAN7.

are a single β-cell population, lacking of the local paracrine cross-talks that are important for appropriate GSIS. For example, it has been reported recently that α-cells facilitate GSIS through glucagon/GLP-1-dependent signalling pathways.[30] Therefore, it is possible that defects in exocytosis (as the consequence of *TSPAN7* KD) could

FIGURE 5 *TSPAN7* KD affects exocytosis from human pancreatic β-cells. (a) Gene expressions that changed significantly in human *TSPAN7* KD pseudo-islet. Volcano plot shows that genes involved in the pathways of secretion (yellow area) and regulation of transport (green area) were down-regulated; markers of the apoptotic pathway (blue) were up-regulated. *TSPAN7* KD was demonstrated by the marked reduction in *TSPAN7* expression (red). (b) Dynamic insulin secretion measured from perifused human pseudo-islets of *TSPAN7* KD (red) or control (Scramble, black) in response to different glucose concentrations and $20\,mM\,K^+$ as indicated. Inset: area of the curve (AUC) of insulin secretion stimulated by $20\,mM\,K^+$. $N = 3$ for control and *TSPAN7* KD, $*p < 0.05$ versus insulin secretion at 1 mM glucose in the same group of pseudo-islets; $^†p < 0.05$ versus control (Scramble), Student's t-test. (c) Examples of exocytosis of *TSPAN7* KD EndoC-βH1 (red) or control EndoC-βH1 (Scramble, black) triggered by depolarisation from -70 to $0\,mV$ with progressively increasing duration (as indicated). (d) Summary of control (black) and exocytosis (normalised to cell size, fF/pF) in relationship to pulse durations. $N = 10$ cells for control and 11 cells for *TSPAN7* KD EndoC-βH1 cells. (e) The relationship between depolarisation-triggered charge influx and pulse durations of control (black) and *TSPAN7* KD (red) EndoC-βH1 cells. $N = 10$ cells for control and 11 cells for *TSPAN7* KD EndoC-βH1 cells. $*p < 0.05$ versus control, student's t-test. (f) The relationship between charges and exocytosis of control (black) and *TSPAN7* KD (red) EndoC-βH1 cells. Corresponding durations of the pulses are as labelled. $N = 10$ cells for control and 11 cells for *TSPAN7* KD EndoC-βH1 cells. (g) Insulin secretion measured from batch-incubated control (black) and *TSPAN7* KD (red) EndoC-βH1 cells in response to 1 and 20 mM glucose. Data are the summary of three independent biological repeats in technical triplicate. $*p < 0.05$ and $***p < 0.001$ versus control insulin secretion at 1 mM glucose and $^{††}p < 0.01$ versus control insulin secretion at 20 mM glucose; two-way ANOVA and Tuckey post hoc test. (h) Insulin content measured from control (black) and *TSPAN7* KD (red) EndoC-βH1 cells. Data are the summary of three independent biological repeats in technical triplicate. All data are presented as mean value ± SEM.
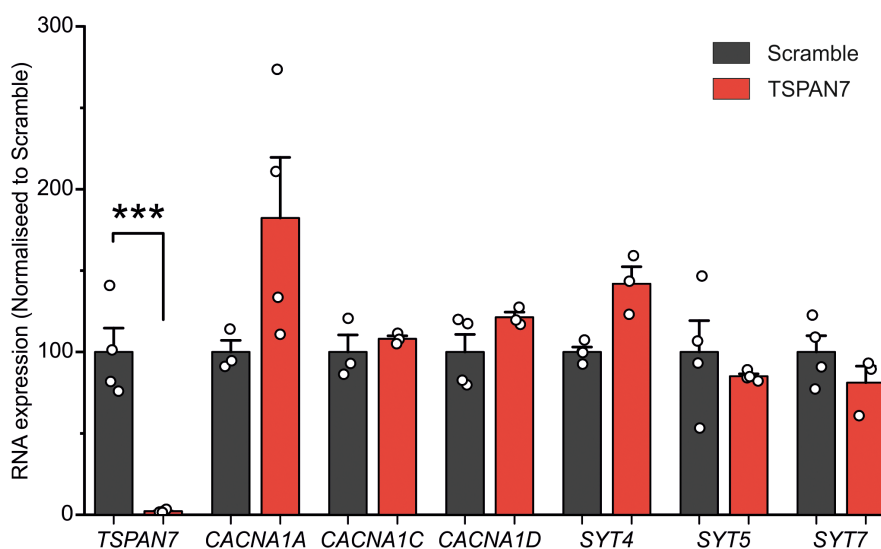

FIGURE 6 Changes in VGCC- and synaptotagmin-encoding genes in EndoC-βH1 following *TSPAN7* KD. The expression of genes encoding TSPAN7 (*TSPAN7*), VGCCs (*CACNA1A*, *CACNA1C* and *CACNA1D*) and synaptotagmins (*SYT4*, *SYT5* and *SYT7*) measured from control (transduced with Ad-Scramble, Scramble, black) and *TSPAN7* KD (red) EndoC-βH1 cells. The levels of expression are normalised to that in control cells (as 100%). Error bars of the control cells condition reflect the variation of the control across the biological repeats. Data are summary of measurements made in two to four independent biological replicates. $***p < 0.0001$ versus control, Student's t-test.

exert a stronger effect in EndoC-βH1 cells. It will be interesting to test whether a significantly reduced GSIS can be also observed in *TSPAN7* KD pseudo-islet composed by pure human primary β-cells.

TSPAN7 knockdown related transcription change is not restricted to exocytotic pathways. There is a small but significant up-regulation of genes involved in apoptosis. It is possible this is due to augmented VGCC activity and secondary to elevated cytosolic Ca^{2+}, which is pro-apoptotic (reviewed in[24]). However, the degree of up-regulation in apoptosis-related genes may not be sufficient

to reduce β-cell mass in either acute or chronic *TSPAN7* loss of function, as evidenced by the normal islet insulin content in *shTSPAN7* transduced EndoC-βH1 cells and in aged Tspan7$^{y/-}$ mice.

In summary, in addition to its inhibitory role on β-cell VGCCs, we found that Tspan7 is required for appropriate expression of genes involved in cell survival and exocytosis. The non-apparent metabolic phenotype and normal GSIS found in Tspan7$^{y/-}$ mice may be the result of a combined effect of enhanced VGCC activity and reduced sensitivity of exocytosis to Ca^{2+} in β-cells.

CONFLICT OF INTEREST

The authors do not have any relevant conflict of interest to disclose.

DATA AVAILABILITY STATEMENT

RNA-sequencing data are available at the NCBI Gene Expression Omnibus (GEO) under the reference number of GSE213731. All functional data are available upon request made to the authors.

ORCID

Quan Zhang https://orcid.org/0000-0002-3626-4855

REFERENCES

1. McLaughlin KA, Richardson CC, Ravishankar A, et al. Identification of Tetraspanin-7 as a target of autoantibodies in type 1 diabetes. *Diabetes*. 2016;65(6):1690-1698. doi:10.2337/db15-1058
2. Eisenbarth GS. Type I diabetes mellitus. A chronic autoimmune disease. *N Engl J Med*. 1986;314(21):1360-1368. doi:10.1056/nejm198605223142106
3. Kitadokoro K, Bordo D, Galli G, et al. CD81 extracellular domain 3D structure: insight into the tetraspanin superfamily structural motifs. *EMBO J*. 2001;20(1–2):12-18. doi:10.1093/emboj/20.1.12
4. Seigneuret M, Delaguillaumie A, Lagaudriere-Gesbert C, Conjeaud H. Structure of the tetraspanin main extracellular domain. A partially conserved fold with a structurally variable domain insertion. *J Biol Chem*. 2001;276(43):40055-40064. doi:10.1074/jbc.M105557200
5. Hemler ME. Tetraspanin functions and associated microdomains. *Nat Rev Mol Cell Biol*. 2005;6(10):801-811. doi:10.1038/nrm1736
6. Bassani S, Cingolani LA. Tetraspanins: interactions and interplay with integrins. *Int J Biochem Cell Biol*. 2012;44(5):703-708. doi:10.1016/j.biocel.2012.01.020
7. Maecker HT, Todd SC, Levy S. The tetraspanin superfamily: molecular facilitators. *FASEB J*. 1997;11(6):428-442.
8. Uhlen M, Fagerberg L, Hallstrom BM, et al. Proteomics. Tissue-based map of the human proteome. *Science*. 2015;347(6220):1260419. doi:10.1126/science.1260419
9. Murru L, Vezzoli E, Longatti A, et al. Pharmacological modulation of AMPAR rescues intellectual disability-like phenotype in Tm4sf2−/y mice. *Cereb Cortex*. 2017;27(11):5369-5384. doi:10.1093/cercor/bhx221
10. Abidi FE, Holinski-Feder E, Rittinger O, et al. A novel 2 bp deletion in the TM4SF2 gene is associated with MRX58. *J Med Genet*. 2002;39(6):430-433. doi:10.1136/jmg.39.6.430
11. Menager MM. TSPAN7, effector of actin nucleation required for dendritic cell-mediated transfer of HIV-1 to T cells. *Biochem Soc Trans*. 2017;45(3):703-708. doi:10.1042/BST20160439
12. Kwon JO, Lee YD, Kim H, et al. Tetraspanin 7 regulates sealing zone formation and the bone-resorbing activity of osteoclasts. *Biochem Biophys Res Commun*. 2016;477(4):1078-1084. doi:10.1016/j.bbrc.2016.07.046
13. Dickerson MT, Dadi PK, Butterworth RB, et al. Tetraspanin-7 regulation of L-type voltage-dependent calcium channels controls pancreatic beta-cell insulin secretion. *J Physiol*. 2020;598(21):4887-4905. doi:10.1113/JP279941
14. Gopel S, Zhang Q, Eliasson L, et al. Capacitance measurements of exocytosis in mouse pancreatic alpha-, beta- and delta-cells within intact islets of Langerhans. *J Physiol*. 2004;556(Pt 3):711-726. doi:10.1113/jphysiol.2003.059675
15. Basco D, Zhang Q, Salehi A, et al. alpha-cell glucokinase suppresses glucose-regulated glucagon secretion. *Nat Commun*. 2018;9(1):546. doi:10.1038/s41467-018-03034-0
16. Lyon J, Spigelman A, MacDonald P, Manning J. *ADI IsletCore protocols for the isolation. Assessment and cryopreservation of human pancreatic islets of langerhans for research purposes v1 (protocols io x3mfqk6)*. 2019
17. Yu Y, Gamble A, Pawlick R, et al. Bioengineered human pseudo-islets form efficiently from donated tissue, compare favourably with native islets in vitro and restore normoglycaemia in mice. *Diabetologia*. 2018;61(9):2016-2029. doi:10.1007/s00125-018-4672-5
18. Hastoy B, Godazgar M, Clark A, et al. Electrophysiological properties of human beta-cell lines EndoC-betaH1 and -betaH2 conform with human beta-cells. *Sci Rep*. 2018;8(1):16994. doi:10.1038/s41598-018-34743-7
19. Kanno T, Rorsman P, Göpel SO. Glucose-dependent regulation of rhythmic action potential firing in pancreatic β-cells by k(ATP)-channel modulation. *J Physiol*. 2002;545(Pt 2):501-507. doi:10.1113/jphysiol.2002.031344
20. Briant LJ, Zhang Q, Vergari E, et al. Functional identification of islet cell types by electrophysiological fingerprinting. *J R Soc Interface*. 2017;14(128):20160999.
21. Robinson MD, McCarthy DJ, Smyth GK. edgeR: a Bioconductor package for differential expression analysis of digital gene expression data. *Bioinformatics*. 2010;26(1):139-140. doi:10.1093/bioinformatics/btp616
22. Lindskog C, Asplund A, Engkvist M, Uhlen M, Korsgren O, Ponten F. Antibody-based proteomics for discovery and exploration of proteins expressed in pancreatic islets. *Discov Med*. 2010;9(49):565-578.
23. Murru L, Ponzoni L, Longatti A, et al. Lateral habenula dysfunctions in Tm4sf2−/y mice model for neurodevelopmental disorder. *Neurobiol Dis*. 2021;148:105189. doi:10.1016/j.nbd.2020.105189
24. Orrenius S, Zhivotovsky B, Nicotera P. Regulation of cell death: the calcium-apoptosis link. *Nat Rev Mol Cell Biol*. 2003;4(7):552-565. doi:10.1038/nrm1150
25. Arvan P, Pietropaolo M, Ostrov D, Rhodes CJ. Islet autoantigens: structure, function, localization, and regulation. *Cold Spring Harb Perspect Med*. 2012;2(8). doi:10.1101/cshperspect.a007658
26. Lebrun P, Atwater I. Effects of the calcium channel agonist, BAY K 8644, on electrical activity in mouse pancreatic B-cells. *Biophys J*. 1985;48(6):919-930. doi:10.1016/S0006-3495(85)83855-8

27. Gut A, Kiraly CE, Fukuda M, Mikoshiba K, Wollheim CB, Lang J. Expression and localisation of synaptotagmin isoforms in endocrine beta-cells: their function in insulin exocytosis. *J Cell Sci*. 2001;114(Pt 9):1709-1716. doi:10.1242/jcs.114.9.1709

28. Yap EL, Greenberg ME. Activity-regulated transcription: bridging the gap between neural activity and behavior. *Neuron*. 2018;100(2):330-348. doi:10.1016/j.neuron.2018.10.013

29. Braun M, Ramracheya R, Bengtsson M, et al. Voltage-gated ion channels in human pancreatic β-cells: electrophysiological characterization and role in insulin secretion. *Diabetes*. 2008;57(6):1618-1628.

30. Zhu L, Dattaroy D, Pham J, et al. Intraislet glucagon signaling is critical for maintaining glucose homeostasis. *JCI Insight*. 2019;4(10). doi:10.1172/jci.insight.127994

SUPPORTING INFORMATION

Additional supporting information can be found online in the Supporting Information section at the end of this article.

How to cite this article: McLaughlin K, Acreman S, Nawaz S, et al. Loss of tetraspanin-7 expression reduces pancreatic β-cell exocytosis Ca^{2+} sensitivity but has limited effect on systemic metabolism. *Diabet Med*. 2022;39:e14984. doi: 10.1111/dme.14984